ELSEVIER

Electroencephalography and clinical Neurophysiology 103 (1997) 395–404

Extraction of ocular artefacts from EEG using independent component analysis

Ricardo Nuno Vigário*

Laboratory of Computer and Information Science, Helsinki University of Technology, P.O. Box 2200, FIN-02015, Hut, Finland

Accepted for publication: 12 March 1997

Abstract

Eye activity is one of the main sources of artefacts in EEG and MEG recordings. A new approach to the correction of these disturbances is presented using the statistical technique of independent component analysis. This technique separates components by the kurtosis of their amplitude distribution over time, thereby distinguishing between strictly periodical signals, regularly occurring signals and irregularly occurring signals. The latter category is usually formed by artefacts. Through this approach, it is possible to isolate pure eye activity in the EEG recordings (including EOG channels), and so reduce the amount of brain activity that is subtracted from the measurements, when extracting portions of the EOG signals. © 1997 Elsevier Science Ireland Ltd.

Keywords: EEG; EOG; Ocular artefact correction; Independent component analysis (ICA); Blind source separation (BSS)

1. Introduction

Among the many sources of artefacts in EEG studies, eye activity plays a dominant role. The need of ocular artefact correction has been shown in the past, and several methods have been introduced (for reviews see, e.g. Brunia et al. (1989) and Jervis et al. (1988)).

The simplest and eventually most commonly used eye artefact correction method is rejection. It is based on discarding portions of EEG that correspond to EOG channel(s) containing attributes (e.g. amplitude peak, variance and slope) that exceed a determined criterion threshold (Barlow, 1979; Verleger, 1993). However, the rejection method may lead to a significant loss of data, as well as leading to the portions used not being representative of the study made. This is particularly important when the brain signals of interest occur near/during strong eye activity, as happens for example in visual tracking experiments.

Another problem associated with the rejection technique is that one may be unable to identify all eye activity beforehand, rejecting only the small portion that one can see, and considering artefact-free what is in fact only artefact-reduced. This may lead to wrong appreciation of the signals observed.

To reduce the presence of eye activity in EEG measurements, the subject is often asked to avoid blinking, fix the eyes on a target, or restrict the blinking at particular times. The effectiveness of this eye fixation method can be questionable, specially in studies of children and of psychiatric or neurological patients, who are not fully co-operative. Thus it may be difficult to collect a sufficient amount of artefact-free data. Besides, this requirement constitutes a secondary task, leading to reduced amplitudes in the task of interest (Weerts and Lang, 1973; Verleger, 1991).

A third class of methods, that could be called EOG subtracting methods, bases its action on the assumption that the measured EEG is a linear combination of true EEG and ocular artefact. Accepting that one or more EOG derivations well represent all eye activity, a correction is proposed by subtraction of a regressed portion of this signal throughout the EEG (see Gratton et al. (1983) for more details). However, as the EOG signal contains a certain amount of brain activity, it is expected that this subtraction distorts the shape of the subsequent EEG responses (Jervis et al., 1989).

Berg and Scherg (1994) have introduced another approach for eye artefact correction, a model based on multiple source eye analysis. In this MSEC (multiple source eye

* Tel.: +358 9 4513287; Fax: +358 9 4513277;
email: Ricardo.Vigario@hut.fi

PII S0013-4694(97)00042-4

EEG 96618

correction) approach, ocular artefact correction is performed by subtracting source waveforms defined by the eye activity, rather than proportions of the resulting EOG signals. The source waveforms are calculated from the EEG signal, together with topographic estimations of the propagation of eye activity throughout the head. This method results in considerable eye artefact suppression, but contains some basic restrictions. First, to perform this type of correction one has to choose a set of calibrating data containing eye activity that goes well above the background signals (in this context, the EEG). As stated above, this requirement may be difficult to fulfil. Second, the technique assumes orthogonality of the source vectors, that are a function of the location and orientation of each source, and of some head parameters. It is possible that this solution represents a good approximation to the real conditions, but some further improvements may be necessary, like some independent considerations between each source and the background EEG.

Huotilainen et al. (1995) used the signal-space projection method to identify and remove eye-blink artefacts, with much success. This approach, like that of Berg and Scherg (1994) requires either a prior modelling of the production of the artefact, or a considerable amount of data where the artefact's amplitude is much higher then the EEG or MEG under study. These requirements, as stated above, may be difficult to fulfil.

Inspired by the non-linearity of signal processing in the human brain, Rao and Reddy (1995) introduced a non-linear on-line method to enhance the EEG signals in the presence of ocular artefacts. Their method, using the recursive least squares based on the second-order Volterra filter, has shown good performance, but its non-linearity is still too limited, as it stops at second order statistics (variances and covariances). Mathematical and experimental work prove that higher order statistics may be needed to separate independent signals (Karhunen, 1996; Hyvärinen and Oja, 1997a; Karhunen et al., 1997; and references therein).

This paper introduces a new method to separate brain activity from eye and other artefacts, based on the assumption that the brain and eye activities are anatomically and physiologically separate processes, and that their independence is reflected in the statistical relation between the electrical signals generated by those processes. Even if no limitation seems to exist on the type of artefact that can be extracted, the fact that the ocular ones are the most representative justify their choice as illustration of the method. Independently, Makeig et al. (1996) have recently introduced a comparable application of the independent component analysis (ICA) to EEG signals. Our results seem to be more convincing, due to the use of a more advanced technical implementation of the ICA.

The remainder of the paper will include a brief introduction to the independent component analysis, with a presentation of the algorithm used and some reasons to use this approach. Finally, experimental data are used to illustrate the success of the technique, together with some consideration of its results.

2. Independent component analysis

Independent component analysis is a useful extension of the principal component analysis (PCA) that was developed some years ago in context with blind source separation applications (Jutten and Herault, 1991; Comon, 1994). In PCA, the eigenvectors of the signal covariance matrix $\mathbf{C} = E\{\mathbf{x}\mathbf{x}^T\}$ give the directions of greater variance on the input data $\mathbf{x}$. (All vectors are understood here as column vectors (single column matrices); T denotes the transpose operator changing a row vector to a column format.) The principal components found by projecting $\mathbf{x}$ onto those perpendicular basis vectors are uncorrelated, and their directions orthogonal. This scheme is very efficient in redundancy reduction (or equivalently in source estimation), and can be said to maximize, in the least squares sense, the amount of information spanned by a subset of dimensions of the initial vector.

However, standard PCA is not suited for dealing with non-Gaussian data. Uncorrelation between a set of vectors, being a necessary prerequisite for statistical independence, is not always a synonym to it. Several authors, from the signal processing to the artificial neural network communities, have shown that information obtained from a second order method such as PCA is not enough and higher-order statistics are needed when dealing with the more demanding restriction of independence (Jutten and Herault, 1991; Comon, 1994; Bell and Sejnowski, 1995; Delfosse and Loubaton, 1995; Karhunen et al., 1997). Good tutorials on neural ICA implementations are now available (Karhunen, 1996; Karhunen et al., 1997). The particular algorithm used in this study was presented and derived by Hyvärinen and Oja (1997a), Hyvärinen and Oja (1997b).

2.1. The model

In blind source separation, the original independent sources are assumed to be unknown, and we only have access to their weighted sum. Fig. 1. depicts a block diagram of our procedure for identification (and possible removal) of EEG artefacts, using an independent component model. In this model, the signals recorded in an EEG study (EOG included), shown in Fig. 3, are noted as $x_k(i)$ (i ranging from 1 to L, the number of electrodes used, and k denoting discrete time). Each $x_k(i)$ is expressed as the weighted sum of M independent signals $s_k(j)$, following the expression:

$$x_k(i) = a_{i1}s_k(1) + a_{i2}s_k(2) + \cdots + a_{iM}s_k(M) \tag{1}$$

or, in a more compact notation,

$$\mathbf{x}_k = \sum_{i=1}^{M} \mathbf{a}(i)s_k(i) = \mathbf{A}\mathbf{s}_k \tag{2}$$

where $\mathbf{x}_k = [x_k(1),\ldots,x_k(L)]^T$ is a vector of length L, made up of the L mixtures at discrete time k. In Eq. (2) $s_k(1),\ldots,s_k(M)$ are M zero mean independent source signals, and $\mathbf{A} = [\mathbf{a}(1),\ldots,\mathbf{a}(M)]$ is a constant mixing matrix whose elements a_{ij} are the unknown coefficients of the mixtures. To guarantee $s_k(i)$ to be a zero mean signal, the mean of each $x_k(j)$ can be explicitly extracted before any further processing. In order to perform ICA, it is necessary to have at least as many mixtures as there are independent sources ($L \geq M$). When this relation is not fully guaranteed, and the dimensionality of the problem is high enough, we should expect the first independent components to present clearly the most strongly independent signals, while the last components still consist of mixtures of the remaining signals. In our study, we did expect the ocular and muscular artefacts, being clearly independent from the brain activity, to come out in the first independent components. The remainder of the brain activity (e.g. alpha and theta rhythms) may need some further separation, or a greater number of measuring electrodes.

The mixing matrix $\mathbf{A}$ is a function of the geometry of the sources and the derivations in an EEG recording and the conductivity properties of the brain, cerebrospinal fluid, skull and scalp. Although this matrix is unknown, we assume it to be constant, or slowly changing (to preserve some local constancy).

We will now divide the independent sources into two classes, i.e. eye and brain activities. All other types of artefacts in this presentation are incorporated in the latter class. The only requirement for such a division is that these two types of signals are statistically independent. Due to the physiologically different processes involved in the production of these electric signals, it is reasonable to expect that this requirement is verified (although these signals may, for example, in evoked response studies be time-locked; see Section 6 for some considerations about the validity of this approach). Eq. (2) then becomes

$$\mathbf{x}_k = \sum_{i=1}^{NB} \mathbf{a}(i)s_k(i) + \sum_{i=1}^{NE} \mathbf{e}(i)o_k(i) \quad (3)$$

where NB and NE are the number of brain and eye sources, respectively. $s_k(i)$ are the brain's independent waveforms, and $o_k(i)$ are the waveforms produced by the eye activity; $\mathbf{e}(i)$ are the columns of matrix $\mathbf{A}$ corresponding to $o_k(i)$. It is interesting to notice the resemblance between the expressions above, and the first two equations in the paper of Berg and Scherg (1994). The main difference introduced here is the possibility of non-orthogonality and the requirement of independence between the brain and the eye waveforms.

The problem is now to estimate the independent signals ($s_k(i)$, $o_k(i)$) from their mixtures, or the equivalent problem of finding the separating matrix $\mathbf{B}$ that satisfies (see Eq. (2)).

$$\hat{\mathbf{s}}_k = \mathbf{B}\mathbf{x}_k \quad (4)$$

In our algorithm, the solution uses the statistical definition of fourth-order cumulant or kurtosis that, for the ith source signal, is defined as

$$kurt(s(i)) = E\{s(i)^4\} - 3[E\{s(i)^2\}]^2 \quad (5)$$

where $E(s)$ denotes the mathematical expectation of s. The kurtosis is negative for source signals whose amplitude has sub-Gaussian probability densities (distributions flatter than Gaussian, positive for super-Gaussian) sharper than Gaussian, and zero for Gaussian densities.

2.2. The algorithm

The initial step in source separation, using the method described in this article, is the whitening, or sphering. This projection of the data is used to achieve the uncorrelation between the solutions found, which is a prerequisite of statistical independence (Hyvärinen and Oja, 1997a). The whitening can also be seen to ease the separation of the independent signals (Karhunen et al., 1997). It may be accomplished by PCA projection, which can be seen in a matricial notation as (see Fig. 1 for graphical explanation of the variables used):

$$\mathbf{v} = \mathbf{V}\mathbf{x}$$

with $E\{\mathbf{v}\mathbf{v}^T\} = I$, where I denotes the unit matrix. The whitening matrix $\mathbf{V}$ is given by

$$\mathbf{V} = \mathbf{\Lambda}^{-1/2}\mathbf{\Xi}^T$$

where $\mathbf{\Lambda} = \mathrm{diag}[\lambda(1),\ldots,\lambda(M)]$ is a diagonal matrix with the eigenvalues of the data covariance matrix $E\{\mathbf{x}_k\mathbf{x}_k^T\}$, and $\mathbf{\Xi}$ is a matrix with the corresponding eigenvectors as its columns.

Consider a linear combination $y = \mathbf{w}^T\mathbf{v}$ of the sphered data vector $\mathbf{v}$, with $\|\mathbf{w}\| = 1$. Then $E\{y^2\} = 1$ and $kurt(y) = E\{y^4\} - 3$, whose gradient with respect to $\mathbf{w}$ is $4E\{\mathbf{v}(\mathbf{w}^T\mathbf{v})^3\}$.

Based on this, Hyvärinen and Oja (1997a) introduced a very simple and highly efficient fixed-point algorithm for computing ICA, calculated over sphered zero-mean vectors $\mathbf{v}$, that is able to find one of the rows of the separating matrix $\mathbf{B}$ (noted $\mathbf{w}$) and so identify one independent source at a time; the corresponding independent source can then be found using Eq. (4). This algorithm, a gradient descent over the kurtosis, is defined, for a particular k, as

1. Take a random initial vector $\mathbf{w}_0$ of unit norm. Let $l = 1$.
2. Let $\mathbf{w}_l = E\{\mathbf{v}(\mathbf{w}_{l-1}^T\mathbf{v})^3\} - 3\mathbf{w}_{l-1}$. The expectation can be estimated using a large sample of $\mathbf{v}_k$ vectors (e.g. 1000 vectors) by computing over successive time points of the EEG.
3. Divide $\mathbf{w}_l$ by its norm (e.g. the Euclidean norm $\|\mathbf{w}\| = \sqrt{\sum_i w_i^2}$).
4. If $|\mathbf{w}_l^T\mathbf{w}_{l-1}|$ is not close enough to 1, let $l = l + 1$ and go back to step 2. Otherwise, output the vector $\mathbf{w}_l$.

In order to estimate more than one solution, and up to a maximum of M, the algorithm may be run as many times as

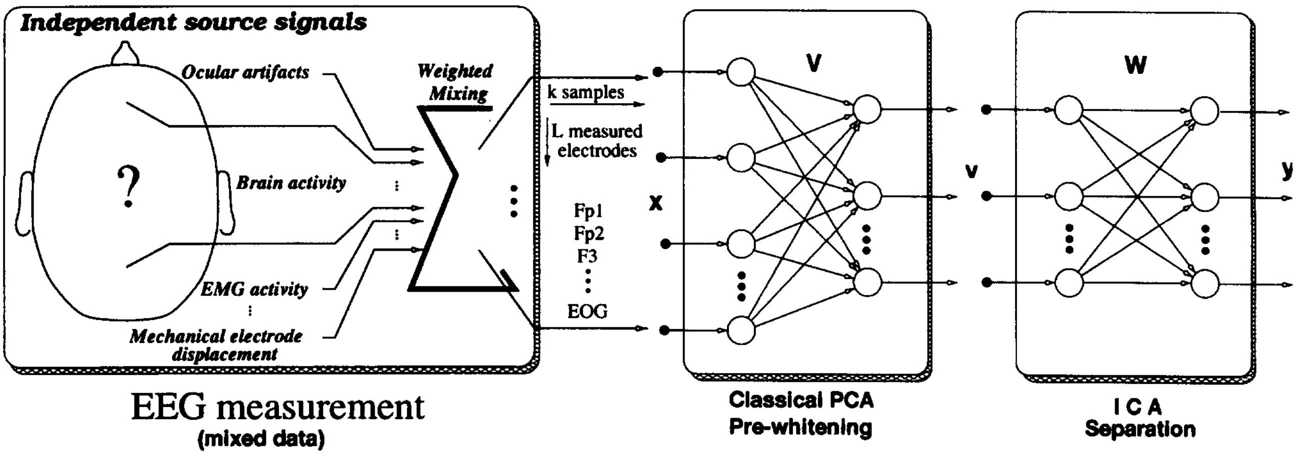

Fig. 1. Block diagram of artifact extraction from EEG, using independent component analysis.

required. It is, nevertheless, necessary to remove the information contained in the solutions already found, to estimate each time as a different independent component. This can be achieved, after the fourth step of the algorithm, by simply subtracting the estimated solution $\hat{s} = \mathbf{w}^T\mathbf{v}$ from the unsphered data $\mathbf{x}_k$. As the solution is defined up to a multiplying constant, the subtracted vector must be multiplied by a vector containing the regression coefficients over each vector component of $\mathbf{x}_k$.

Considering **A** to be constant, **B** will also be kept unchanged throughout successive sections of the EEG recordings.

Due to the cubic convergence of the algorithm (Hyvärinen and Oja, 1997a), the solution is typically found in less than 15 iterations.

3. Simulated data

To give an illustrative example of the behaviour of the model presented, consider the case of Fig. 2a,b. Three signals are shown, presenting all extreme distributional behaviour of the kurtosis. $S1$ is an epileptic discharge-like signal, with very sharp amplitude distribution and high positive kurtosis, $S2$ is white noise, with a Gaussian distribution and zero kurtosis and $S3$ is a sinusoid, with near-to-flat distribution and strong negative kurtosis (this fourth moment is not limited in the positive direction, but has a negative bound at −2).

After mixing the signals, all resulting sequences have close to Gaussian distributions (Fig. 2c,d). As could be expected, the PCA projection (also called whitening, as it forces all directions of the transformed data to have equal variance (see the algorithm section for a method to perform this transformation)) was able to deal with the only Gaussian signal, and could get some of the positive kurtotic signal out (see the projections $W1$ and $W2$ of Fig. 2e). However, the complete separation of the independent signals can only be achieved in the last frame of Fig. 2, when the ICA projection is performed. A qualitative look at the solutions $ICA1 \ldots ICA3$ (Fig. 2g), together with the quantitative appreciation of their distributions (Fig. 2h) show how close these time sequences are to the original ones (Fig. 2a).

The ICA solutions can thus be found through maximization of the absolute value of the kurtosis of a linear combination of the observed signals (maximizing for positive kurtotic combinations, and minimizing for negative ones).

4. Experimental data

The experimental data used in this paper were taken from the study of Joutsiniemi et al. (1995). A routine clinical 22-channel EEG was recorded for 15–25 min from children aged 9–13 years. During the recording, the subjects were lying with their eyes closed, and a few times they were asked to open and close their eyes. They were not prevented from falling asleep. The training set input to the ICA algorithm consisted of a subset of 5 min of EEG, visually inspected to guarantee the presence of eye activity. The records of all subjects showed results agreeing with the example presented in this paper.

The 22 electrodes were placed according to the international 10-20 system, as shown on the last frame of Fig. 5, and were all referred to C_z. A 23rd electrode was just above the right eye, between the eyelid and the eyebrow, and was referred to F_{p1} to measure EOG. This EOG montage is not a typical one, as it only reflects some slight vertical and

Fig. 2. Examples of independent source signals with positive, zero and negative kurtosis values (a), their amplitude distributions (b), and the respective value for the kurtosis below this last figure. The mixtures of the previous signals (c) have near to zero kurtosis and close to Gaussian distributions (d). From PCA projection (e,f) to ICA (g,h) the resulting time series have clearer negative, positive or zero kurtosis values close to those of the initial independent source signals.

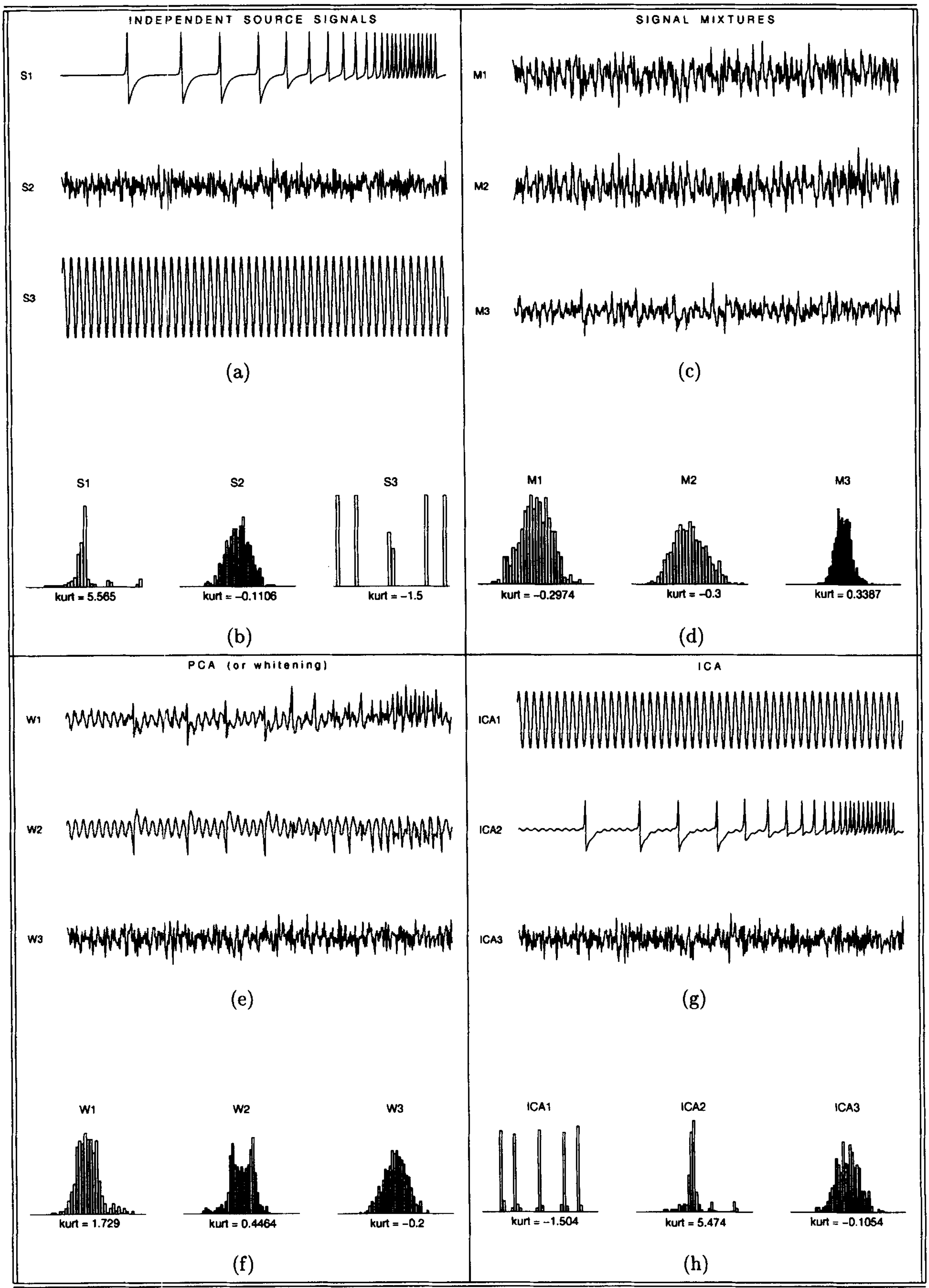
INDEPENDENT SOURCE SIGNALS
S1
S2
S3
(a)
SIGNAL MIXTURES
M1
M2
M3
(c)
S1
S2
S3
kurt = 5.565
kurt = -0.1106
kurt = -1.5
(b)
M1
M2
M3
kurt = -0.2974
kurt = -0.3
kurt = 0.3387
(d)
PCA (or whitening)
W1
W2
W3
(e)
ICA
ICA1
ICA2
ICA3
(g)
W1
W2
W3
kurt = 1.729
kurt = 0.4464
kurt = -0.2
(f)
ICA1
ICA2
ICA3
kurt = -1.504
kurt = 5.474
kurt = -0.1054
(h)

horizontal gradients, but it was nevertheless useful for the identification and validation of the independent components found. It is important to note here that a separate EOG channel should not even be necessary to isolate the eye activity. It can be expected that eye artefacts present in the 22 scalp electrodes are extractable due to their independence from the brain's activities (some preliminary analysis of data without any EOG channel support this expectation).

All signals were digitally band-pass filtered from 0.1to 25 Hz, and then down-sampled from 200 to 50 Hz.

Fig. 3 shows the 6th, the earlier half of the 8th, and the 10th minutes of one subject's record, respectively noted as *I*, *II* and *III*. These sections were selected to show some structures that appeared in the first few independent components.

Section *I* presents strong eye activity, evident in the frontal electrodes (F_{p1}, F_{p2} and F_{pz}), as well as in the EOG channel. The first 15 s in F_8 show some eye blinking that was not captured by the EOG channel which illustrates the suboptimal use of possible EOG information (note that this EEG measurement was not tailored to illustrate the usefulness of ICA in ocular artefact correction). The duration of the deflections (0.3 s and 0.1 s) are a good signature of blinking type of activity.

Section *II* of the figure shows strong and very local activity in channel T_3, evidently due to mechanical electrode movement. C_3 and F_7 show some coinciding activity that could be due to filter adaptation response. Electrodes T_4 and F_8 reveal high-frequency muscle activity during section *III*.

5. Results

As an illustration of the separation abilities of ICA algorithms, the first eight independent components found from the EEG study are plotted in Fig. 4. Some of the waveforms shown are actually multiplied by −1 to ease the visual comparison with the EEG data in Fig. 3. ICA solutions are defined up to a multiplying constant that cannot be estimated with this technique. The real scaling factor of each component is found by regression through each electrode on the scalp (see Fig. 5 and the explanations at the end of this section).

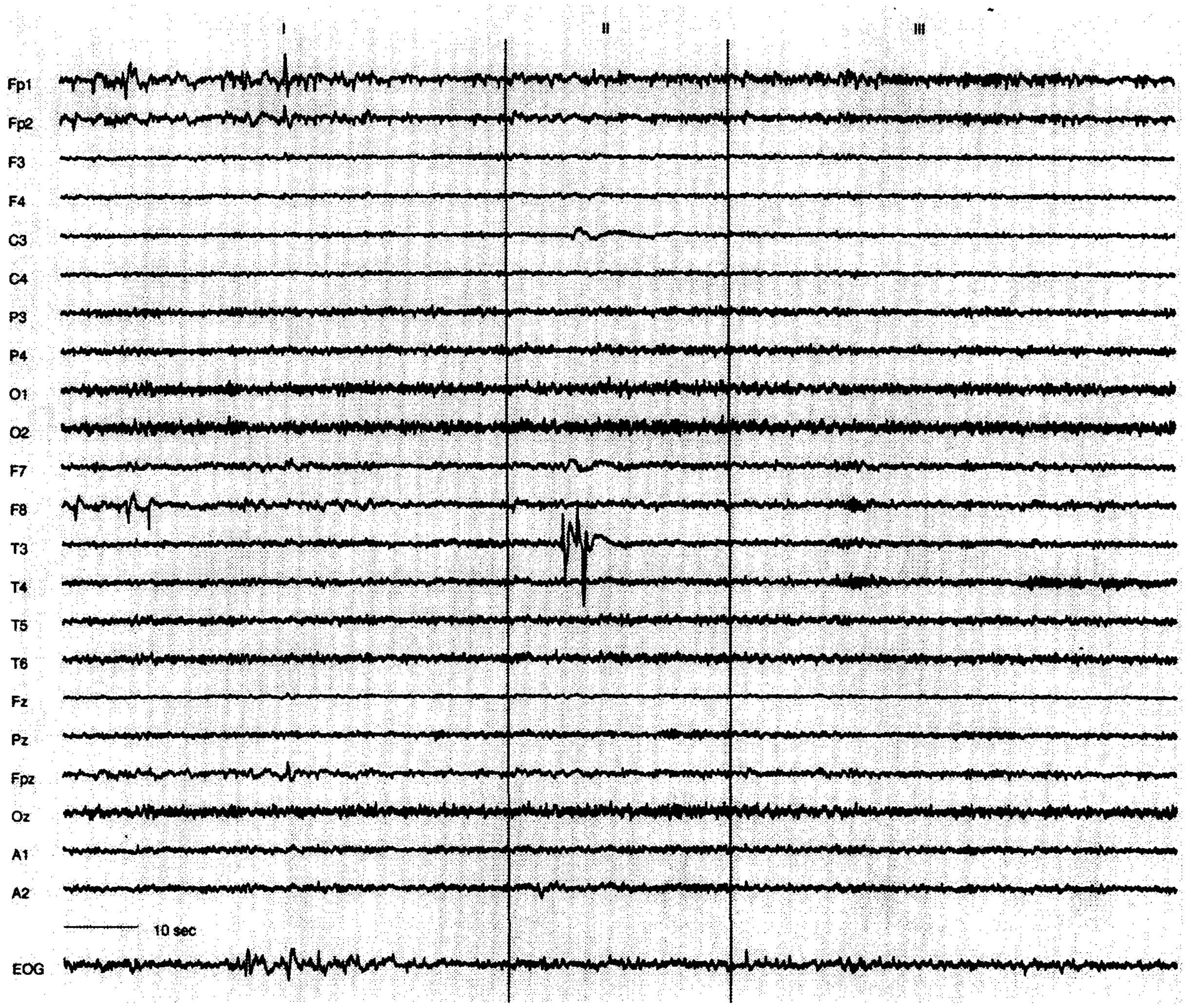

Fig. 3. Three sections of the same EEG record, corresponding to the 6th minute of measurement, the early half of the 8th, and the 10th minute, respectively noted as sections *I*, *II* and *III*.

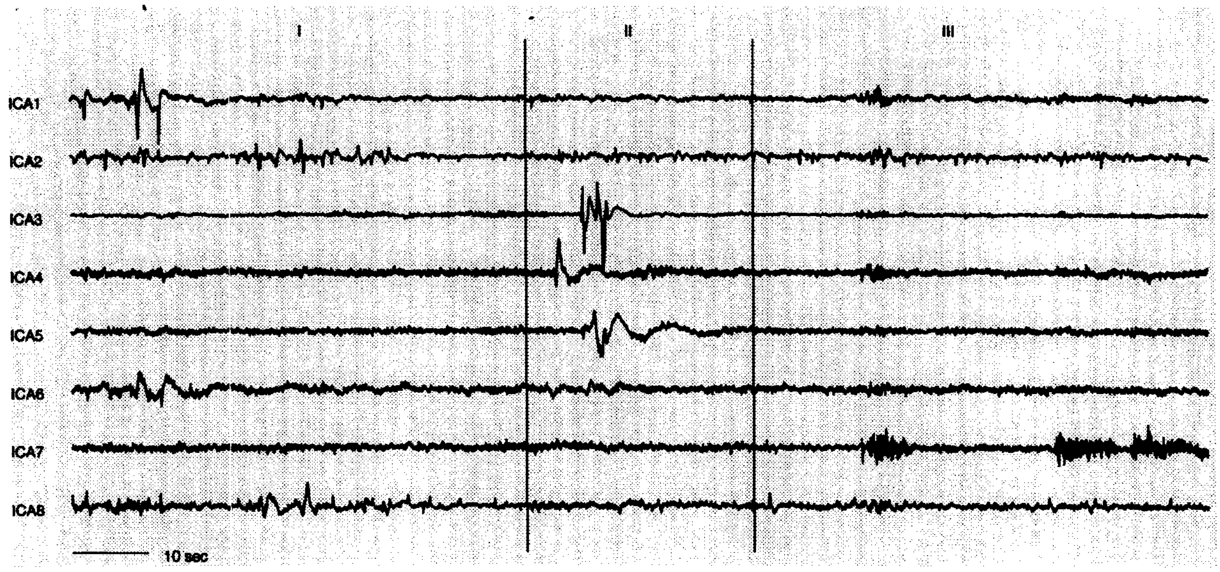

Fig. 4. First eight ICA components for the three sections of Fig. 3.

The eye blinking on channel $F8$ was clearly isolated in the first ICA component, reducing even the fluctuation around the blinks, enhancing the signal-to-noise ratio of the channel (everything that is not directly related to the blinks is considered here noise). The comparison of respective signals in Figs 3 and 4 shows that the background oscillations have similar amplitude while the peaks are over twice as strong in the latter.

*ICA*2 and *ICA*8 together span the activity present in the EOG channel. Please note again the clean signal in *ICA*2, when compared, e.g. with F_{p1} or EOG signals of Fig. 3. Fig. 6 gives a closer look at these solutions. The mechanical disturbance in T_3 appears in *ICA*3, and the electronic adaptation triggered by it in *ICA*5. The usefulness of ICA in EEG analysis is very strongly shown in section *II* of the 4th component, where a clear signal appears with no visible EEG deflection. In fact, A_2 displays a small coinciding bump, but it is embedded in much stronger brain activity. Finally, *ICA*7 shows bursts of high frequency oscillations (visible in T_4 and F_8), due to electromyographic activity, completely isolated.

As stated above, ICA solutions are defined up to a multiplying constant. To find out the right constant that brings the solution close to its representation for each EEG signal, linear regression may be used. Fig. 5 depicts the coefficients of that regression, for each one of the first eight solutions (each component in a separate frame). The inspection of the diagrams indicates the topographic importance of the respective ICA solution throughout the scalp. It should be recalled that all electrodes were referred to C_z, which explains why no data are present at the vertex.

The area of each hexagon is proportional to the amplitude of the regression parameter, and the two grey shades correspond to the positive and negative signs.

The distribution in *Regr*4, together with the shape of *ICA*4 in Fig. 4, leads us to suggest that *ICA*4 reflects a K-complex, generated at the vertex during the initialization of sleep.

Frames *Regr*2 and *Regr*8 (the frames corresponding to the ICA solutions containing eye activity) indicate that *ICA*2 was found by computing a horizontal gradient on the scalp electrode signals (from *Regr*2 it is clear that the average of the frontal left-hand electrical signals is extracted from the right-handed average, in order to produce the second ICA component), while *ICA*8 was attained through a vertical gradient on the referred signals (in *Regr*8 the subtraction is made between the average of the frontal signals and the EOG (please remember that the EOG channel is measured from above the right eye to F_{p1})). This may reflect the different behaviour of vertical and horizontal components of eye movements.

Fig. 6a zooms to section *I* of Fig. 3 for the frontal electrodes F_{p1}, F_{p2}, F_{pz} and the EOG channel. The influence from *ICA*1 was subtracted from all signals to avoid unnecessary confusion when comparing some ICA solutions with the EOG. Fig. 6b has the 2nd and 8th ICA components, together with their weighted sum (with weights defined by the coefficients of their regression on the EOG channel), and the residual of the subtraction of the sum from the EOG signal.

One can clearly inspect the structures in *ICA*2 and *ICA*8 in a more detailed way than in the EEG signals. The residual signal, obtained by subtracting the solutions from the EOG, has a considerable magnitude and may still carry some meaningful brain activity. In traditional ocular artefact removal, when subtracting a portion of the full EOG signal from the EEG, the signal noted as residual is also used, even if it does not seem to carry any information on eye activity, but rather on other physiological brain functions. The regular oscillations in the parieto-occipital electrodes P_3, P_4, O_1, O_2 and O_z, with typical alpha frequency of 7–10 Hz, although present in considerable amounts throughout all the

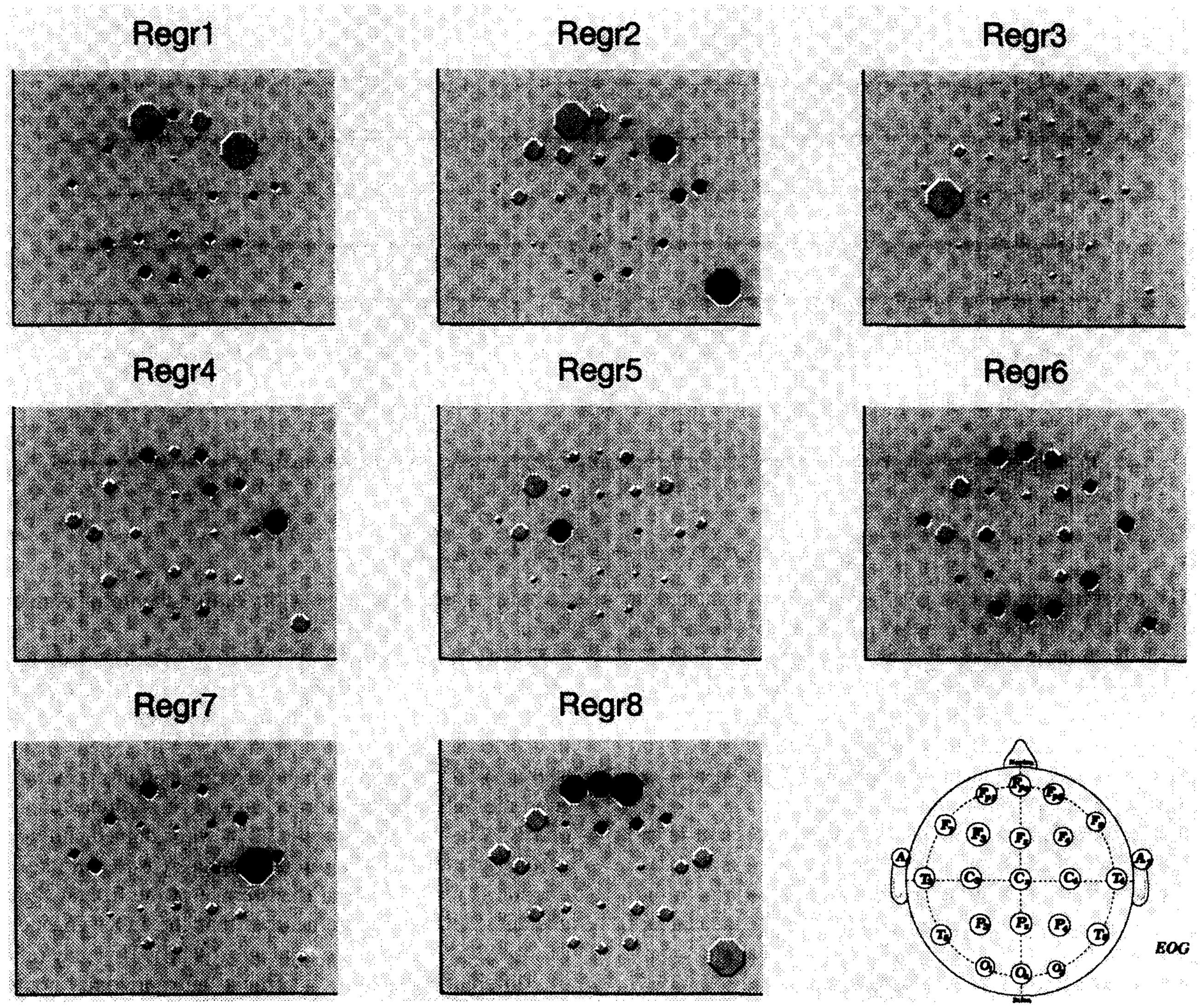

Fig. 5. Scalp distribution of the regression coefficients corresponding to the eight ICA components shown in the previous figure. The area of each hexagon is proportional to the amplitude of the regression coefficient, and the grey shade tells its sign. The positions of the hexagons correspond to the electrode locations, as shown on the last frame.

measurement, just appeared among the last independent components, and will not be reported in this paper.

6. Discussion

The present paper introduced a new approach to ocular artefact cancellation from EEG recordings, based on the statistical technique of independent component analysis. This method was initially tested in some simulated data, showing very good performance in the separation of signals from their linear mixtures. In experimental data, ICA was able to extract the eye information present in the EOG signals, and use this information in the removal of this type of artefact, rather than the complete EOG (that still has some remaining brain activity). This technique seems to be an improvement to the traditional artefact cancelling methods.

As stated in the introductory section of this paper, the basic assumption made on the data used in the study is that of independence between brain and artefact waveforms. In most cases this independence is verified due to the differences in physiological origins of those signals. Nevertheless, in some event-related potential (ERP) studies (e.g. using infrequent or painful stimulus), both the cerebral and ocular signals can be similarly time-locked to the stimulus. This time dependence, present only for a very short instant, may be of some limitation in these particular studies. However, as the independence between two signals is a measure of the similarity between their joint amplitude distribution and the product of each signal's distribution (calculated throughout the entire signal, and not only close to the stimulus applied), it can be expected that the very local relation between those two signals, during stimulation, will not affect their global statistical relation.

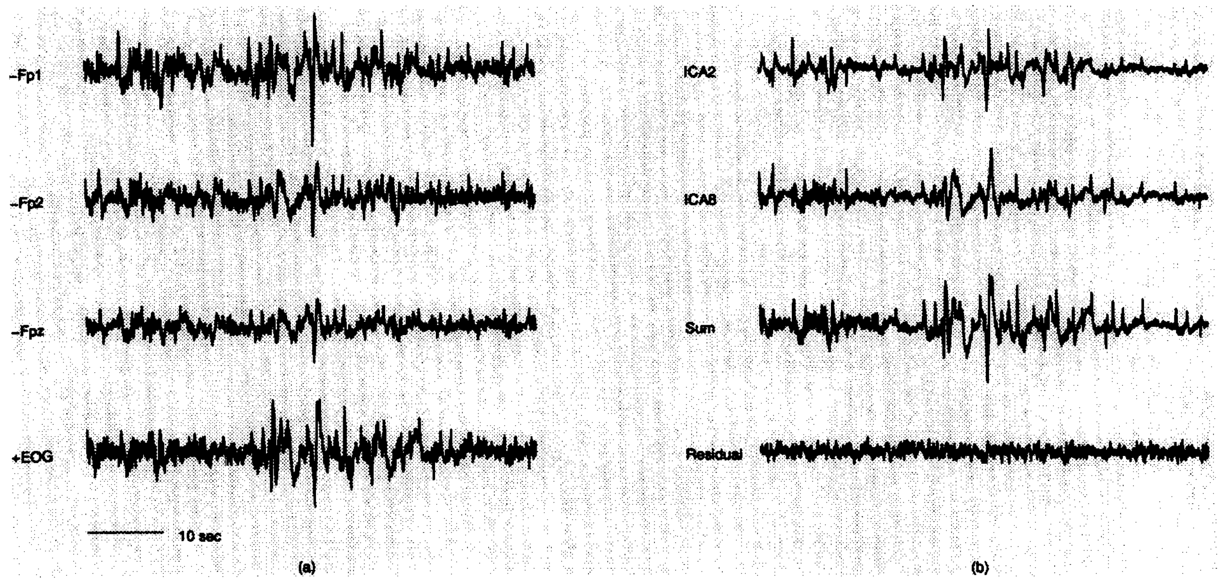

Fig. 6. (a) Expanded section *I* of Fig. 3 for the frontal and the EOG channels. (b) ICA components 2 and 8, their weighted sum (with the coefficients defined by regression on the EOG channel), and the residual of the subtraction of the sum from the EOG signal for the same time period.

It should be noted that the ICA method is not yet an attempt to fully automate the detection and removal of artefacts from the EEG data, but rather a potentially helpful tool that will be available to the EEG community. Combination of this method with other automatic feature extractors may lead to the required automation.

Since eye activity is intrinsically independent from the background EEG, due to its origins, no theoretical limitation exists to the use of this method without any EOG channel. Nevertheless, the use of EOG information is advisable, as it tunes the search for eye activity, and helps in validating between eye artefact and other classes of disturbances.

More than one EOG channel may be included in further experiments to better tune the search for a more accurate description of the eye artefacts. Elbert et al. (1985) have suggested the use of three EOG channels; one vertical, one lateral and one radial.

Furthermore, the ICA method may, with small changes, take into account other sorts of artefacts, e.g. muscle activity or mechanical displacement of electrodes. It can be expected that this method still holds for the analysis of certain brain activities (e.g. detection of alpha and theta rhythms, decomposition of ERP complexes, etc.).

Acknowledgements

The author thanks Professor Riitta Hari and Professor Erkki Oja for their comments on the manuscript, Mr Aapo Hyvärinen for technical support in the ICA algorithm and for indispensable discussions on the experiments reported, Dr Lea Leinonen for help in the interpretation of the EEG data, and two anonymous reviewers for their helpful suggestions. The author holds a grant from JNICT, under its Programa PRAXIS XXI.

References

Barlow, J.S. Computerized clinical electroencephalography in perspective. IEEE Trans. Biomed. Eng., 1979, 26: 377–391.

Bell, A. and Sejnowski, T. An information-maximization approach to blind separation and blind deconvolution. Neural Computation, 1995, 7: 1129–1159.

Berg, P. and Scherg, M. A multiple source approach to the correction of eye artifacts. Electroenceph. clin. Neurophysiol., 1994, 90: 229–241.

Brunia, C.H.M., Möcks, J. and den Berg-Lennsen, M.V. Correcting ocular artifacts – a comparison of several methods. J. Psychophysiol., 1989, 3: 1–50.

Comon, P. Independent component analysis – a new concept?. Signal Processing, 1994, 36: 287–314.

Delfosse, N. and Loubaton, P. Adaptive blind separation of independent sources: a deflation approach. Signal Processing, 1995, 45: 59–83.

Elbert, T., Lutzenberger, W., Rockstroh, B. and Niels Birbaumer, N. Removal of ocular artifacts from the EEG – a biophysical approach to the EOG. Electroenceph. clin. Neurophysiol., 1985, 60: 455–463.

Gratton, G., Coles, M. and Donchin, E. A new method for off-line removal of ocular artifact. Electroenceph. clin. Neurophysiol., 1983, 55: 468–484.

Huotilainen, M., Ilmoniemi, R.J., Tiitinen, H., Lavaikainen, J., Alho, K., Kajola, M. and Näätänen, R. The projection method in removing eye-blink artefacts from multichannel MEG measurements. In: C. Baumgartner, L. Deecke, G. Stroink and S.J. Williamson (Eds.), Biomagnetism: Fundamental Research and Clinical Applications (Proc. 9th Int. Conf. Biomag.), Elsevier, Amsterdam, 1995, pp. 363–367.

Hyvärinen, A. and Oja, E. A fast fixed-point algorithm for independent component analysis. Neural Computation, 1997a, in press.

Hyvärinen, A. and Oja, E. One-unit learning rules for independent component analysis. In: Neural Information Processing Systems 9 (Proc. NIPS'96). MIT Press, Cambridge, MA, 1997b.

Jervis, B.W., Ifeachor, E.C. and Allen, E.M. The removal of ocular artifacts from the electroencephalogram: a review. Med. Biol. Eng. Comput., 1988, 26: 2–12.

Jervis, B.W., Coelho, M. and Morgan, G. Effect on EEG responses of removing ocular artifacts by proportional EOG subtraction. Med. Biol. Eng. Comput., 1989, 27: 484–490.

Joutsiniemi, S.-L., Kaski, S. and Larsen, T.A. Self-organizing map in recognition of topographic patterns of EEG spectra. IEEE Trans. Biomed. Eng., 1995, 42: 1062–1068.

Jutten, C. and Herault, J. Blind separation of sources, part i: and adaptive algorithm based on neuromimetic architecture. Signal Processing, 1991, 24: 1–10.

Karhunen, J. Neural approaches to independent component analysis and source separation. In: Proceedings of the 4th European Symposium on Artificial Neural Networks (ESANN'96), Bruges, Belgium, 1996.

Karhunen, J., Oja, E., Wang, L., Vigário, R. and Joutsensalo, J. A class of neural networks for independent component analysis. IEEE Trans. Neural Networks, 1997, 8: 486–504.

Makeig, S., Bell, A., Jung, T.-P. and Sejnowski, T. Independent component analysis of electroencephalographic data. In: Neural Information Processing Systems 8 (Proc. NIPS'95). MIT Press, Cambridge, MA, 1996.

Rao, K.D. and Reddy, D.C. On-line method for enhancement of electroencephalogram signals in presence of electro-oculogram artifacts using nonlinear recursive least squares technique. Med. Biol. Eng. Comput., 1995, 33: 488–491.

Verleger, R. The instruction to refrain from blinking affects auditory p3 and n1 amplitudes. Electroenceph. clin. Neurophysiol., 1991, 78: 240–251.

Verleger, R. Valid identification of blink artifacts: are they larger than 50 μv in EEG records?. Electroenceph. clin. Neurophysiol., 1993, 87: 354–363.

Weerts, T.C. and Lang, P.J. The effects of eye fixation and stimulus and response location on the contingent negative variation (cnv). Biol. Psychol., 1973, 1: 1–19